Tectonic features on the lunar south pole

Tectonic activities on planetary bodies are studied regularly to understand the complex nature of the planets interior. For e.g., during the movement of the crustal plates on the Earth topographic variations are observed resulting into geomorphological features that are mapped by rigorous field investigations and supported by remotely sensed data. The information content generated through various sensors including microwave sensors are inferred from spatial platforms. The current study uses Narrow Angle Camera (NAC) and Wide Angle Camera (WAC) data from LRO mission and m-chi decomposition images derived from Mini- SAR data from Chandrayaan-1 to infer the presence of crustal tectonic activity in the south polar region of the moon (Figure.1) [Mukherjee and Singh, 2014].

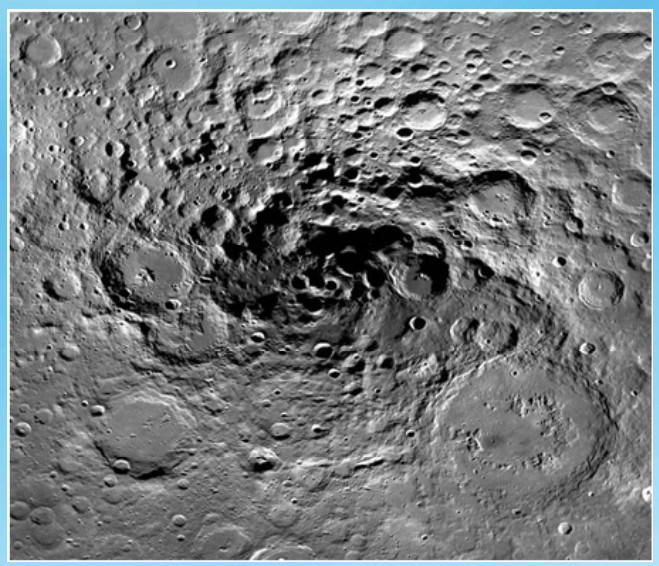

Figure.1. South Polar region of the Moon [Wide Angle Camera Image Mosaic from LRO]

Mini-SAR imaging radar on-board Chandrayaan-1 mission was the first mono-static lunar orbiting synthetic aperture radar. Mini-SAR data is primarily used to identify signatures suggesting the possibility of the presence of water ice within the permanently shadowed regions of the lunar poles. Further, this data has been used to observe various other geological features such as melt flows, crater ejecta blankets, secondary craters etc (Mukherjee and Singh, 2015, Saran et al, 2014). Therefore, identification of distinct morphological features in the shadowed as well as illuminated regions of lunar surfaces can be easily done using mini-SAR data. The SAR technology can also penetrate the surface and therefore is an effective tool to look for hidden fault lines in the shadowed portions on the lunar regolith (Mukherjee and Singh, 2015).

The Mini-SAR data strips each having four bands were downloaded from NASA Planetary Data system (PDS) node. The S-band mini-SAR radar data has a resolution of 150 m/ pixel [Saran et al., 2013]. The relevant data strips were projected and mosaiced using ISIS software. Each pixel in an image strip consists of 16 bytes data in four channels of 4 bytes each as |LH|2, |LV|2, Real (LH.LV*) and Imaginary (LH.LV*). The first two channels represent the intensity images of the'horizontal' and 'vertical' receive, respectively. The last two channels represent the real and imaginary components respectively of the complex value for the cross power intensity image between 'horizontal' and 'vertical' receive. This data was then used for deriving Stokes vectors (Mukherjee and Singh, 2015). Mini-SAR data has a phase shift of 45° in the anticlockwise direction which exaggerates the number of pixels showing volume backscattering [Mohan et al., 2011]. Therefore, phase calibration was done for Band 3 and Band 4 using the following band math equations on ENVI software:

$$\mathrm{Re}(LH\ LV^*)_{calib} = \mathrm{Re}(LH\ LV^*)\cos 45° - lm(LH\ LV^*)\sin 45° \quad (1)$$

$$lm(LH\ LV^*)_{calib} = \mathrm{Re}(LH\ LV^*)\sin 45° + lm(LH\ LV^*)\cos 45° \quad (2)$$

Stokes Parameters (S_0,S_1,S_2,S_3) were calculated using Bands 1 and 2 and phase calibrated Bands 3 and 4 for each data strip using the equations in (3) as described in [Spudis et al., 2010]:

$$S = \begin{bmatrix} S_0 = \langle |E_{LH}|^2 + |E_{LV}|^2 \rangle \\ S_1 = \langle |E_{LH}|^2 - |E_{LV}|^2 \rangle \\ S_2 = 2\Re e\langle E_{LH}.E^*_{LV} \rangle \\ S_3 = -2\Im m\langle E_{LH}.E^*_{LV} \rangle \end{bmatrix} \quad (3)$$

Equations from Saran et al, 2012 were used to calculate the degree of polarization (m) and CPR. Equations from Raney, 2012 and Raney, 2012 were used to calculate the degree of circularity (χ) and m-χ scattering contributions for each pixel on ENVI software. The equations used are as follows:

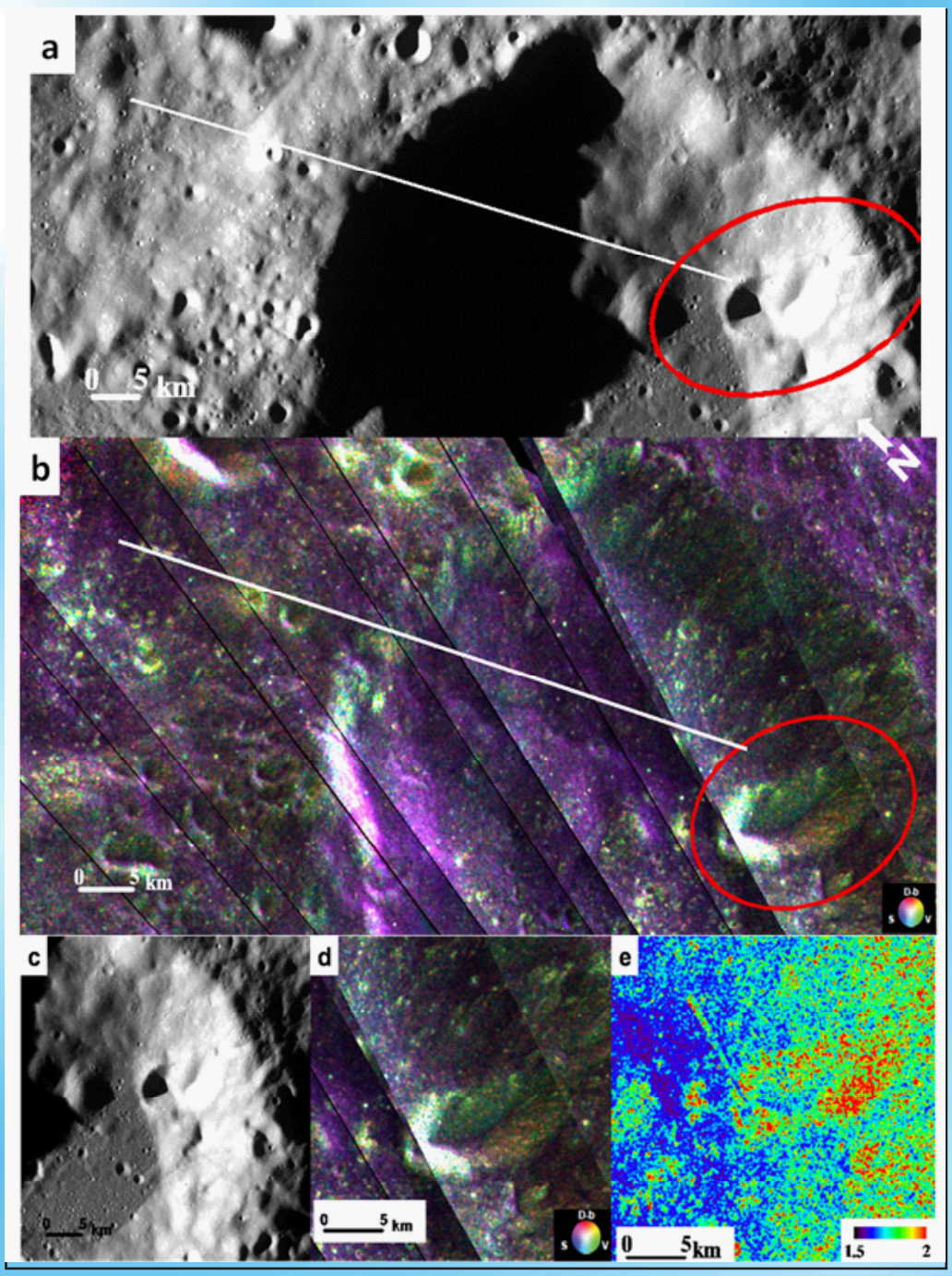

Figure 2. a) WAC image of the partially shadowed region of the Cabeus B crater floor in the lunar south pole. b) m-chi decomposition image of the fault running within Cabeus B crater and beyond. c) WAC image of the debris avalanche possibly triggered from movement along the identified fault. d) m-chi decomposition image of the debris avalanche. e) CPR image of the debris avalanche showing the surface roughness. [Figure Ref. Mukherjee and Singh, 2015; fig 4].

$$m = \sqrt{\{(S_1)^2 + (S_2)^2 + (S_3)^2\}} / S_0 \quad (4)$$

$$CPR = (S_0 - S_3) / (S_0 + S_3) \quad (5)$$

$$Sin\ 2c = -S_3 / (m * S_0) \quad (6)$$

$$B = \sqrt{\{(S_0) * m * [1 - \sin(2c)]\} / 2} \quad (7)$$

$$G = \sqrt{\{(S_0) * (1 - m)\}} \quad (8)$$

$$R = \sqrt{\{(S_0) * m * [1 + \sin(2c)]\} / 2} \quad (9)$$

Here blue (B) in (7) indicates single-bounce (Bragg) backscattering, green (G) in (8) represents the randomly polarized constituent or volume scattering and red (R) in (9) corresponds to double–bounce scattering.

M-χ decomposition images display a false colour composite showing "blue" for surface scattering, "red" for double bounce scattering and "green" for volume/diffuse scattering. The images obtained along with optical data (Wide Angle Camera with 100m/ pixel resolution from LROC) were used to study the surface features in and around the identi-

fied craters within the South Polar Region of the moon.

Earlier studies have tried to study the deformational features such as faults and grabens on the lunar crust and compared them to similar features present on the Earth (Schwarz, 1928). Another study observed the presence of compressional and extensional features such as lobate scarps and grabens on the farside lunar highlands that are indicative of recent crustal tectonic activity (Watters et al, 2014). Dasgupta et al., 2014, have also found features within a rille, Rima Hyginus, located on the near side of the lunar surface, showing horizontal displacement of crustal blocks indicative of some shear stress. The findings in this study also suggest the manifestation of crustal tectonic activity on the moon in the form of faults and grabens due to the above mentioned forces. Previous studies investigating lunar tectonic activity have used optical data primarily to study lunar tectonics. Present work confirms that partially and completely shadowed crater interiors present in the Polar Regions can also contain unique features indicative of tectonic activity using microwave sensor data such as mini-SAR.

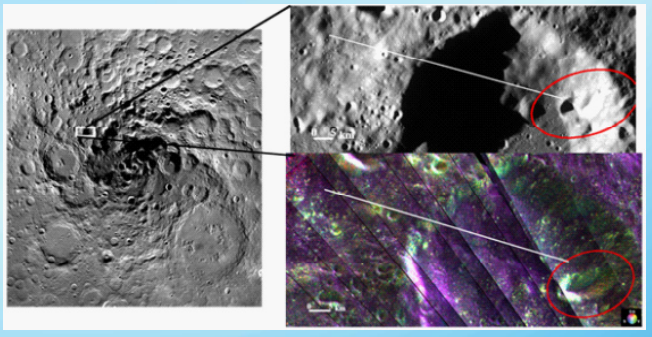

Figure 3. Region in the south polar region of the moon having the fault and the debris avalanche.

It has been proposed that thermal stress may also have been responsible for the lineaments observed on the lunar lithosphere. Such lineaments are tectonic landforms which indicate the occurrence of subsurface geological perturbations as a result of dislocation along fault planes resulting in surface disruptions, evidence of which gets buried over time under the lunar regolith or degraded due to space weathering [Anand et, al. 2004]. M-χ decomposition of Mini-SAR data [Patterson et al 2012] has therefore been used to demarcate such hidden lineaments and associated dislocation features in the study region (Figure 2, 3).

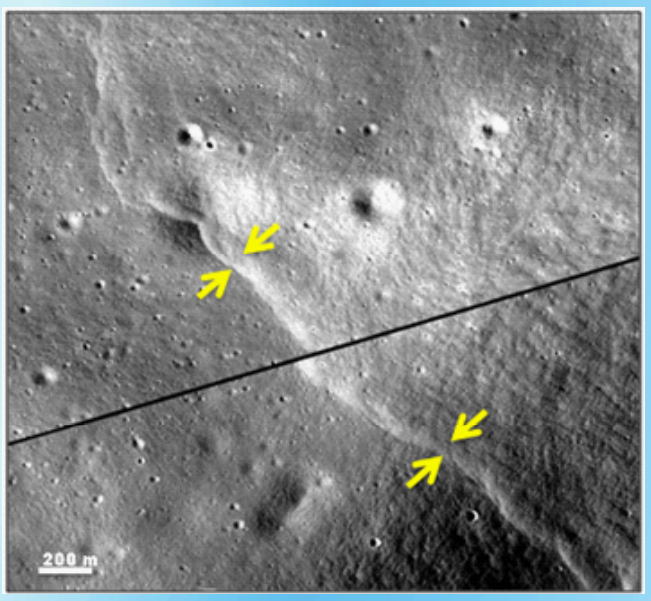

Figure 4. Inferred Lunar Fault developed by recent compressional crustal tectonic activity lying between Boltzman and Doerfel Craters within the lunar south polar region using Narrow Angle Camera images. [Figure Ref. Mukherjee and Singh, 2015; fig. 2d]

The structural geological information observed in the form of scarps, faults and the associated debris avalanches observed on the surface of the Moon suggests present and past tectonic activities on this satellite. These structural features are comparable with the features of the Earth. This investigation is useful in view of future manned and unmanned lunar investigation and suitable landing sites for future scientific investigations of the Moon. Crustal tectonic activity therefore helps to demarcate regions experiencing physical and geological stress within the planetary interior. The geological activity and the related geodynamics lead to the formation of unique features suitably addressed as the surface manifestations of underlying subsurface perturbations. The formation of such tectonic features derived from perturbations along faults is suggestive of the recent crustal movement of the lunar body. Also, the shallow (<100 km depth) moonquakes recorded on Apollo data could have resulted due to activity along such type of tectonic deformations present at different locations on the lunar surface [Nakamura et al., 1979]. The inferred crustal dislocation features reported in this paper suggest that the lunar interior could be seismically active and that further geological perturbations as such can be expected [Figure 4].

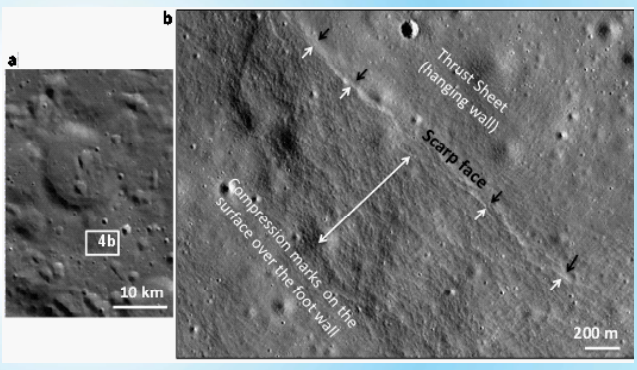

Figure 5. Compression marks on Scarp segment. a, Wide Angle Camera image of the scarp region. b, Narrow Angle Camera Image of a segment of the inferred scarp marked in a showing compression marks on the surface of the foot wall of the thrust fault.[Figure ref. Mukherjee and Singh, 2015; fig. 3]

Furthermore, the use of radar data can reveal hidden tectonic land deformations possibly formed due to disturbances along the subsurface faults. Application of m-χ decomposition technique on mini-SAR data effectively helps to demarcate fault lines in shadowed as well as illuminated regions underneath the lunar regolith due to the unique capability of microwaves to penetrate the regolith, completely independent of solar illumination. Therefore, using SAR data and the derived parameters, several complex lineament systems portraying the tectonic peculiarities of a region can be identified. The study region should be focused more using a fine resolution and deeper penetrating radar sensor or a ground based rover with ground penetrating radar to study the uniqueness of the underlying geodynamics of the south polar lunar surface and derive comparisons with other polar and equatorial regions (Mukherjee and Singh, 2014).

Further reading/References:

1. Anand, M.,Taylor,L.A.,Nazarov,M.A.,Shu,J.,Mao,H.-K.,Hemley,R.J.,2004.Space weathering on airless planetary bodies: clues from the lunar mineral hapkeite. Proc. Natl. Acad. Sci. USA 101, 6847–6851. http://dx.doi.org/10.1073/pnas.0401565101.

2. Dasgupta, N., Ruj, T., Das, A. and Saran, S.,2014. Horizontal forces within lunar crust: Intriguing a questioning mind. 45th Lunar and Planetary Science Conference 2014. Abstract 1343.

3. Mukherjee, S. and Singh P., 2014. Application of m-χ decomposition technique on Mini-SAR data to understand crater and ejecta morphology, IEEE Geoscience and Remote Sensing letters, vol. 12, no.1, pp. 73-76.

4. Mukherjee, S. & Singh, P., 2014. Investigation of tectonic processes in the lunar South Polar Region using Mini-SAR and other data. Front. Earth Sci. doi:10.3389/feart.2014.00006 fert.2014 00006 (Nature Publishing Group).

5.Mukherjee,S. & Singh,P., 2015. Identification of tectonic deformations on the south polar surface of the moon. Planetary and Space Science, Elsevier. http://dx.doi.org/10.1016/j.pss.2015.04.010i.

6. Nakamura, Y. et al. 1979. Shallow moonquakes: Depth, distribution and implications as to the present state of the lunar interior. Proc. lunar Sci. Conf. , 2299-2309.

7. Spudis, P.D. et al., 2010. Initial results for the north pole of the moon from mini-SAR, Chandrayaan-1 mission, Geophys. Res. Lett., vol. 37, no. 6.

8. Patterson, G.W., Raney, R.K., Cahill, J.T.S. & Bussey, D.B.J., Characterization of lunar crater ejecta deposits using m-chi decompositions of mini-RF data. Proc. Eur. Planetary Sci. Congr. 7, 731, (2012). pp. 159–164, 2011.

9. Raney, R.K., Cahill, J.T.S., Patterson, G.W. and Bussey, D. B. J., 2012. The m-χ decomposition of hybrid dual-polarimetric radar data, IEEE Int. IGARSS, pp.

Saumitra Mukherjee
Remote Sensing and Space Sciences
School of Environmental Sciences
Jawaharlal Nehru University
E-mail: saumitramukherjee3@gmail.com

Priyadarshini Singh
Remote Sensing Applications Laboratory
School of Environmental Sciences,
Jawaharlal Nehru University
E-mail: ps.sesjnu@gmail.com